

**Cite this article as:** Wang Huigai, Zhang Keke, Wang Bingying, et al. Effect of Ni Modified GNSs on Thermal Aging Characteristics of SnAgCuRE/Cu Soldering Joints[J]. Rare Metal Materials and Engineering, 2024, 53(06): 1523-1535. DOI: 10.12442/j.issn.1002-185X.E20230039.

ARTICLE

# Effect of Ni Modified GNSs on Thermal Aging Characteristics of SnAgCuRE/Cu Soldering Joints

Wang Huigai<sup>1,2</sup>, Zhang Keke<sup>1,2</sup>, Wang Bingying<sup>1</sup>, Wang Yaoli<sup>1,2</sup>

<sup>1</sup>School of Materials Science and Engineering, Henan University of Science and Technology, Luoyang 471023, China; <sup>2</sup>Collaborative Innovation Center of Nonferrous Metals, Henan Province, Provincial and Ministerial Co-construction of Collaborative Innovation Center for Non-ferrous Metal New Materials and Advanced Processing Technology, Luoyang 471023, China

**Abstract:** Sn<sub>2.5</sub>Ag<sub>0.7</sub>Cu<sub>0.1</sub>RE<sub>0.05</sub>Ni lead-free solder alloy was used as the research object. Based on the unique structure, excellent physical properties, and good mechanical properties of graphene nanosheets (GNSs), the Ni modified GNSs (Ni-GNSs) were used as the reinforcement phase. The soldering process of Ni-GNSs reinforced SnAgCuRE system composite solder/Cu and thermal aging tests of soldering joints were conducted to investigate the effect of Ni-GNSs on the microstructure and thermal aging fracture mechanism of composite soldering joints. Results show that the addition of Ni-GNSs inhibits the linear expansion of the composite solder, resulting in lattice distortion and dislocation. The intermetallic compound (IMC) particles near the dislocation line interact with the dislocations and hinder their movement, thereby strengthening the composite solder and further improving the soldering joint. With a longer thermal aging time, the thickness of interface IMC layer is increased and the shear strength of soldering joints is decreased. Among them, the shear strength decrement of the composite soldering joints with 0.05wt% GNS addition is the least of only 8.9%. Moreover, after thermal aging for 384 h, its shear strength is still higher than that of the Sn<sub>2.5</sub>Ag<sub>0.7</sub>Cu<sub>0.1</sub>RE<sub>0.05</sub>Ni/Cu soldering joint before thermal aging. With the addition of Ni-GNSs, the growth coefficient of interface IMC of composite soldering joints is significantly reduced, which effectively alleviates the degradation of mechanical properties of composite solder/Cu soldering joints during the thermal aging process, further changes the thermal aging fracture mechanism of composite solder/Cu soldering joints, and ultimately affects the reliability of joints. The fracture position of the Sn<sub>2.5</sub>Ag<sub>0.7</sub>Cu<sub>0.1</sub>RE<sub>0.05</sub>Ni/Cu soldering joints moves from the soldering seam before thermal aging to the soldering seam/interface IMC, presenting the ductile-brittle mixed fracture. The fracture position of the Sn<sub>2.5</sub>Ag<sub>0.7</sub>Cu<sub>0.1</sub>RE<sub>0.05</sub>Ni-0.05GNSs/Cu soldering joints is still in the soldering seam zone, presenting the ductile fracture, which indicates the high reliability of the soldering joints.

**Key words:** Ni-GNSs/SnAgCuRE system composite solder; interface IMC; soldering joints; thermal aging; microstructure and properties

With the improvement of microelectronic circuit integration, the number of soldering joints on the device is increased, and the size becomes smaller and smaller. The failure of soldering joints will affect the reliability of the device, which mainly depends on the environment and characteristics of the soldering joints. Among them, the influence of heat-mechanical action is more significant. Kim et al<sup>[1]</sup> showed that the heat generated during the service of electronic components promotes the further growth of intermetallic compound (IMC) and production of stress. More

seriously, IMC may be transformed into new phases, which weakens the mechanical properties of the joint to a certain extent and even causes fracture failure.

Among the current lead-free solders, Sn-based lead-free solder has high fatigue resistance, good wettability, and weldability, therefore widely used in the microjoining field<sup>[2-3]</sup>. However, in the process of fine-pitch and high-density packaging, the wettability, strength, and toughness of the current joints are slightly unqualified. In order to further improve the wettability of lead-free solder and to achieve

Received date: September 05, 2023

Foundation item: National Natural Science Foundation of China (U1604132); Key Technology Research and Development Program of Henan Province (222102230114); Major Scientific Research Foundation of Higher Education of Henan Province, China (23B430003)

Corresponding author: Wang Huigai, Ph. D., Associate Professor, School of Materials Science and Engineering, Henan University of Science and Technology, Luoyang 471000, P. R. China, Tel: 0086-379-64231269, E-mail: 9902783@haust.edu.cn

Copyright © 2024, Northwest Institute for Nonferrous Metal Research. Published by Science Press. All rights reserved.

good wettability and soldering connection with substrate materials, composition amelioration of the solder is the most direct and effective method.

In order to widen the application range of Sn5Sb-based materials, such as third-generation semiconductors, in higher-temperature package conditions, Xin et al<sup>[4]</sup> studied the microstructure evolution and mechanical properties of micro-alloyed Sn-5Sb/Cu soldering joints during the isothermal aging process. Results show that the addition of Cu, Ni, Ag, and other alloying elements can effectively inhibit the growth of  $\text{Cu}_6\text{Sn}_5$  compound and generate the fine  $(\text{Cu}, \text{Ni})_6\text{Sn}_5$  and  $\text{Ag}_3\text{Sn}$  compounds. These compounds play a pinning role at the grain boundary, more effectively inhibit the diffusion between the solder and the Cu substrate, and form a finer microstructure and a thinner interface  $\text{Cu}_3\text{Sn}$  layer. Additionally, the precipitation strengthening of alloying elements significantly improves the microhardness of the aging joint, which effectively alleviates the premature deformation and fracture under high temperature service, thereby being conducive to the rapid development of the third-generation semiconductor interconnection materials. Yang et al<sup>[5]</sup> studied the effect of Mo on the microstructure evolution in Sn58Bi-xMo/Cu soldering joints during aging and found that the addition of Mo nanoparticles increases the atomic diffusion activation energy of the composite solder and decreases the diffusion coefficient, thus reducing the growth rate of  $\text{Cu}_6\text{Sn}_5$  layer. Yang et al<sup>[6]</sup> added a trace amount of Ge to Sn-0.7Cu solder to study the interface reaction and mechanical properties of soldering joints during thermal aging and thermal cycling. Results show that the addition of Ge decreases the diffusion rate of Sn and Cu atoms, promotes the formation of SnGe solid solutions, and improves the shear strength of soldering joints. Besides, the thickness of IMC layer at soldering joint interface reduces. The addition of Ge also improves the reliability of the soldering joints during the thermal cycles. In addition to the micro-nano metal particles, the addition of micro-nano ceramic particles also has the same effect<sup>[7]</sup>.

The addition of nano-carbon materials into the lead-free solder can effectively improve the mechanical properties of composite solder and soldering joint due to their fine grain strengthening, pinning, and bridging effects<sup>[8]</sup>. Jiang et al<sup>[9]</sup> studied reliability of graphene nanosheets (GNSs) reinforced Sn-58Bi/Cu soldering joints. Results show that with the addition of GNSs, the shear fracture mode of Sn-58Bi solder converts from brittle fracture into the mixed mode of brittle and ductile fracture, which is coincident with the shear strength variation. Han et al<sup>[10]</sup> studied the interface reaction of GNSs enhanced SAC305 soldering joints during thermal aging at 150 °C, and found that scallop-like interface IMC forms during soldering, and the morphology of IMC changes from scallop-like form to irregular form during thermal aging. After soldering and thermal aging, IMC layer thickness of SAC305/Cu soldering joint is larger than that of composite solder/Cu soldering joint. Compared with solder matrix, the diffusion coefficient of composite soldering joint is reduced, indicating that GNSs can effectively hinder the growth of

interface IMC. However, the nano-carbon material has a large specific surface area and it is easy to agglomerate, which degrades the mechanical properties. After GNSs addition, carbon nanotubes (CNTs) and other carbon-based nanoparticles can be modified by metal. The diffusion between elements becomes a key control factor for the growth of interface IMC during soldering and thermal aging. Jing et al<sup>[11]</sup> analyzed the effect of Ag-GNSs on the IMC growth process of SAC305/Cu soldering joints. Compared with that of SAC305 material, the thickness of IMC layer of composite soldering joints reinforced by Ag-GNSs is significantly smaller, indicating that Ag-GNSs can reduce the diffusion coefficient of interface atoms and inhibit the growth of interface IMC layer. Park et al<sup>[12]</sup> studied the mechanical, electrical, and thermal properties of Sn-58Bi composite soldering joints strengthened by Ag-multi-walled CNTs (MWCNTs) during the thermal aging process and found that the thickness of IMC layer at the soldering joint interface is twice larger than that of the composite soldering joint interface after thermal aging for 1000 h. The composite soldering joint with 0.05Ag-MWCNTs has the optimal shear strength and the small resistivity and thermal resistance.

The formation and microstructure evolution of IMC during the interface reaction between solder material and metal substrate have been widely researched, as well as IMC influence on the mechanical properties and subsequent service performance of soldering joints<sup>[13-17]</sup>. However, the morphology, microstructure of interface IMC, and fracture mechanism of Ni-GNSs reinforced SnAgCuRE (RE indicates the rare earth element) composite solder/Cu soldering joints during thermal aging are rarely reported. GNSs in the composite solder present excellent heat conduction characteristics, and their thermal radiation coefficient is more than 0.95, so it is expected to improve the thermal efficiency of current electronic components and to enhance the service stability of soldering joints.

In this research, the evolution of interface microstructure and mechanical properties of composite solder/Cu soldering joint during thermal aging were analyzed. The formation mechanism, growth dynamics of interface IMC, and failure fracture mechanism of soldering joint were discussed. Then, the mechanism of GNSs in the interface reaction and thermal aging process of composite solder/Cu soldering joint was revealed. The prevention measures for the thermal aging failure of microelectronic package interconnect soldering joints were discussed.

## 1 Experiment

The test material was Sn2.5Ag0.7Cu0.1RE0.05Ni-xGNSs composite solders. According to the addition amount of GNS (0wt% , 0.01wt% , 0.03wt% , 0.05wt% , 0.07wt% , and 0.10wt%) in the composite solder and the composition of the solder matrix (Sn2.5Ag0.7Cu0.1RE0.05Ni), nickel in the composite solder was added in the form of Ni-GNSs. The theoretical nickel loading in Ni-GNSs was calculated according to the amount of GNS added in the composite

solder. The composite solder was prepared by mechanical alloying and rolled into a thin solder strip of 0.1 mm. The to-be-soldered surfaces of the thin solder strip and the Cu substrate were firstly polished with sandpaper and then washed by ultrasonic cleaning machine with acetone. After the removal of oil and oxide impurities on the surface, the composite solder was dried for subsequent use.

The thin strip solder was placed between the lap surfaces of the upper and lower Cu substrates for furnace soldering, as shown in Fig. 1. Based on the optimization results of wettability test parameters, the soldering tests of composite solders with different GNS addition amounts were conducted with washing flux at 270 °C.

The soldering joint was placed in a box resistance furnace for thermal aging test. In order to avoid oxidation of the soldering joint, the sample of the soldering joint was placed in the molybdenum disulfide for thermal aging treatment according to the Japanese test methods<sup>[18]</sup>. The test temperature was 150 °C, which is also the maximum service temperature of microelectronic connection. The thermal aging time was 0, 48, 96, 192, and 384 h. After the thermal aging treatment, the sample of the soldering joint was air-cooled.

The composite solder rod was cut into uniform sheets with the size of  $\Phi 8$  mm $\times$ 0.4 mm. Grind the solder sheets with 1200#–2000# sandpaper until the sheet thickness was about 120  $\mu$ m. Then, punch the sheets into small wafers with the diameter of 3 mm and continuously grind them until the thickness was about 80  $\mu$ m. MTP-1A type electrolysis double spray thinning instrument was used to thin the center thickness of the wafer ( $\Phi 3$  mm). Then, the wafer was put into ethanol immediately for cleaning. Before the observation by transmission electron microscope (TEM), the samples were thinned again with Gatan691 ion thinning instrument to ensure the clean surface. The interface morphology and microstructure of composite solder were characterized by JEM-2100 TEM.

Due to the irregular morphology of IMC layer at the interface of composite soldering joint, the area query method was used to measure the thickness of IMC layer in this research. Firstly, the area of the interface IMC layer was measured with ImageJ software, and then the thickness of the interface IMC layer was obtained by measuring the length. Additionally, ImageJ software was also used to measure the particle size of the interface IMC. A representative field of view was selected to measure the diameter of about 100 IMC particles, and their average value was used as the size of interface IMC particles.

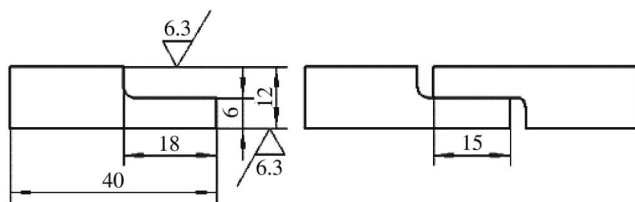


Fig.1 Schematic diagram of soldering joint

## 2 Results and Discussion

### 2.1 Microstructure and structural characterization of Ni-GNSs/SnAgCuRE composite solder

The results in Ref. [8] show that the improvement in reliability of the soldering joint largely depends on the strengthening effect of Ni-GNSs on the composite solder, which is closely related to the microstructure of the composite solder. The composite solders were analyzed by high resolution TEM (HRTEM), selected area electron diffraction (SAED), and energy dispersive spectroscopy (EDS), and the analysis results of composite solder containing 0.05wt% GNSs are shown in Fig.2. In Fig.2a, it can be observed that the black granular material with 30–80 nm in diameter is uniformly distributed on the surface of the light gray material. EDS results of the nanoparticles show that the contents of Ni and C are 5.07at% and 83.98at%, respectively, indicating that the Ni particles exist on the GNS surface. According to SAED pattern, the interplanar crystal spacing of 0.209, 0.171, and 0.113 nm has a good correspondence with the (111), (200), and (311) crystal face spacing of Ni, respectively, which belongs to the  $[02\bar{2}]$  crystal band axis with lattice constant  $a=0.3619$  nm. Because this lattice constant is close to that of standard Ni ( $a=0.3524$  nm), it can be further determined that the nanoparticles are Ni.

Fig. 2d shows the morphology of composite solder. According to EDS analysis results, the bright black particles with the atomic ratio of Ag:Sn=65.24:25.11 are  $Ag_3Sn$ . Two sets of spots can be observed in Fig.2e. The strong spots are the solder alloy spots, and the weak spots are the precipitated phase spots. According to SAED pattern of the bright black particles, the interplanar crystal spacing of 0.492, 0.348, and 0.217 nm has a good correspondence with the crystal face spacing of the  $Ag_3Sn$  (001), (011), and (012) planes, respectively, which belongs to the  $[100]$  crystal band axis. It can be further determined that the bright black particle is  $Ag_3Sn$  (Pmmn space group, lattice constant  $a=0.597$  nm,  $b=0.478$  nm,  $c=5.184$  nm,  $\alpha=\beta=\gamma=90^\circ$ , orthomorph system). According to EDS analysis results of the gray particles marked by the dashed rectangle in Fig.2g (the atomic ratio of Cu to Sn is 41.07:44.12), it is preliminarily determined that the composition of the gray particles is mainly  $Cu_6Sn_5$ . According to SAED pattern, the interplanar crystal spacing of 0.206, 0.163, and 0.122 nm corresponds to the crystal face spacing of  $Cu_6Sn_5$  (020),  $(\bar{1}13)$ , and  $(\bar{1}33)$  planes, respectively, which belongs to the  $[602]$  crystal band axis. These results further prove that the gray particles are  $Cu_6Sn_5$ .

Dislocation lines, dislocation walls, and IMC particles near the dislocation lines can also be observed in the composite solder, as shown in Fig.2j. Due to the small linear expansion coefficient of GNSs<sup>[19]</sup>, the addition of the reinforcement phase Ni-GNSs inhibits the linear expansion of the composite solder<sup>[20]</sup>, resulting in the lattice distortion and eventually dislocation. IMC particles are distributed near the dislocation line. During the dislocation movement, IMC particles interact with the dislocation, hindering the dislocation movement<sup>[21]</sup>. The

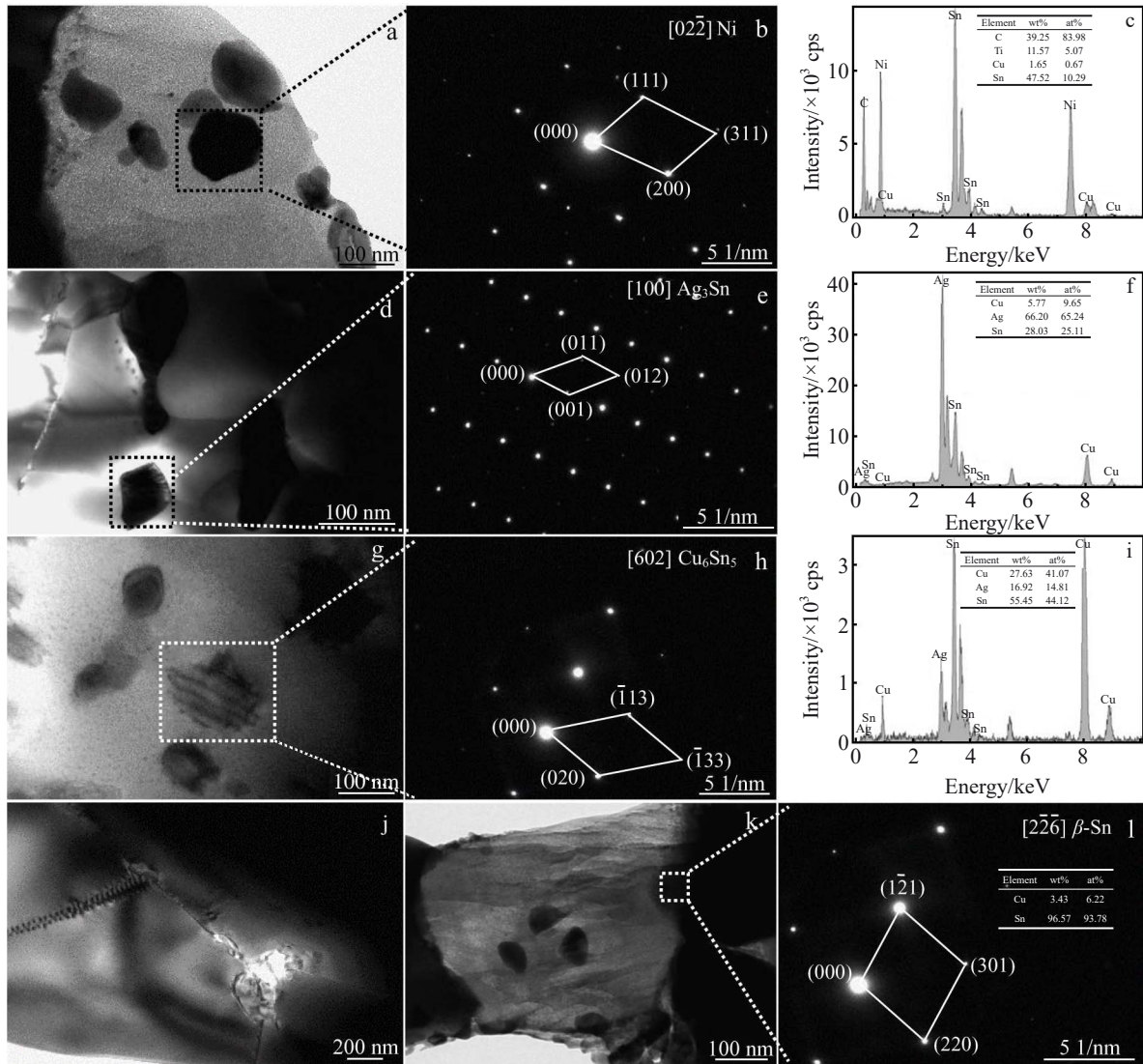


Fig.2 HRTEM images (a, d, g), SAED patterns (b, e, h), and EDS analysis (c, f, i) of Ni (a–c),  $\text{Ag}_3\text{Sn}$  (d–f), and  $\text{Cu}_6\text{Sn}_5$  (g–i) particles in composite solder containing 0.05wt% GNSs; HRTEM image of dislocation in composite solder (j); HRTEM image of Ni-GNSs/ $\beta$ -Sn interface (k); SAED pattern with EDS analysis of  $\beta$ -Sn (l)

dislocation wall in Fig.2j further hinders the dislocation movement, thus increasing the strength of the composite solder.

Fig. 2k shows the interface morphology of Ni-GNSs and composite solder. The middle light gray material is GNSs, and Ni nanoparticles with uniform size of 30–80 nm are distributed evenly on GNS surface, indicating that there is a high bonding between Ni and GNSs. According to EDS analysis results of the black material on both sides (Sn content is 96.57wt%), the black material is preliminarily identified as  $\beta$ -Sn matrix. According to SAED pattern, the interplanar crystal spacing of 0.209, 0.207, and 0.166 nm has a good correspondence with the (220), (1 $\bar{2}$ 1), and (301) crystal face spacing of  $\beta$ -Sn, respectively, which belongs to the [2 $\bar{2}$ 6] crystal band axis. These results further prove that the black material is  $\beta$ -Sn. The bonding surface of Ni-GNSs and  $\beta$ -Sn matrix is smooth and uniform, and there are no cracks and other defects.

Hence, the composite solder is mainly composed of  $\beta$ -Sn,

$\text{Ag}_3\text{Sn}$ , and a small amount of  $\text{Cu}_6\text{Sn}_5$ , and defects, such as dislocation lines and dislocation walls, exist in the composite solder. Some IMC particles are distributed near the dislocation lines, which hinders the dislocation movement and strengthens the composite solder. The interface of Ni-GNSs and solder alloy is well bonded, and no cracks and other defects can be observed.

## 2.2 Microstructure evolution of composite solder/Cu soldering joint during thermal aging

Fig.3 shows the interface morphologies of soldering joints with different GNS additions after thermal aging at 150 °C for different durations. It can be observed that thickness of IMC layer is increased with the prolongation of aging time. In addition to the scalloped IMC, there is also a small amount of prismatic IMC, and the roughness of IMC layer increases firstly and then decreases. After thermal aging for 384 h, a thicker  $\text{Cu}_3\text{Sn}$  layer appears below the  $\text{Cu}_6\text{Sn}_5$  layer at the

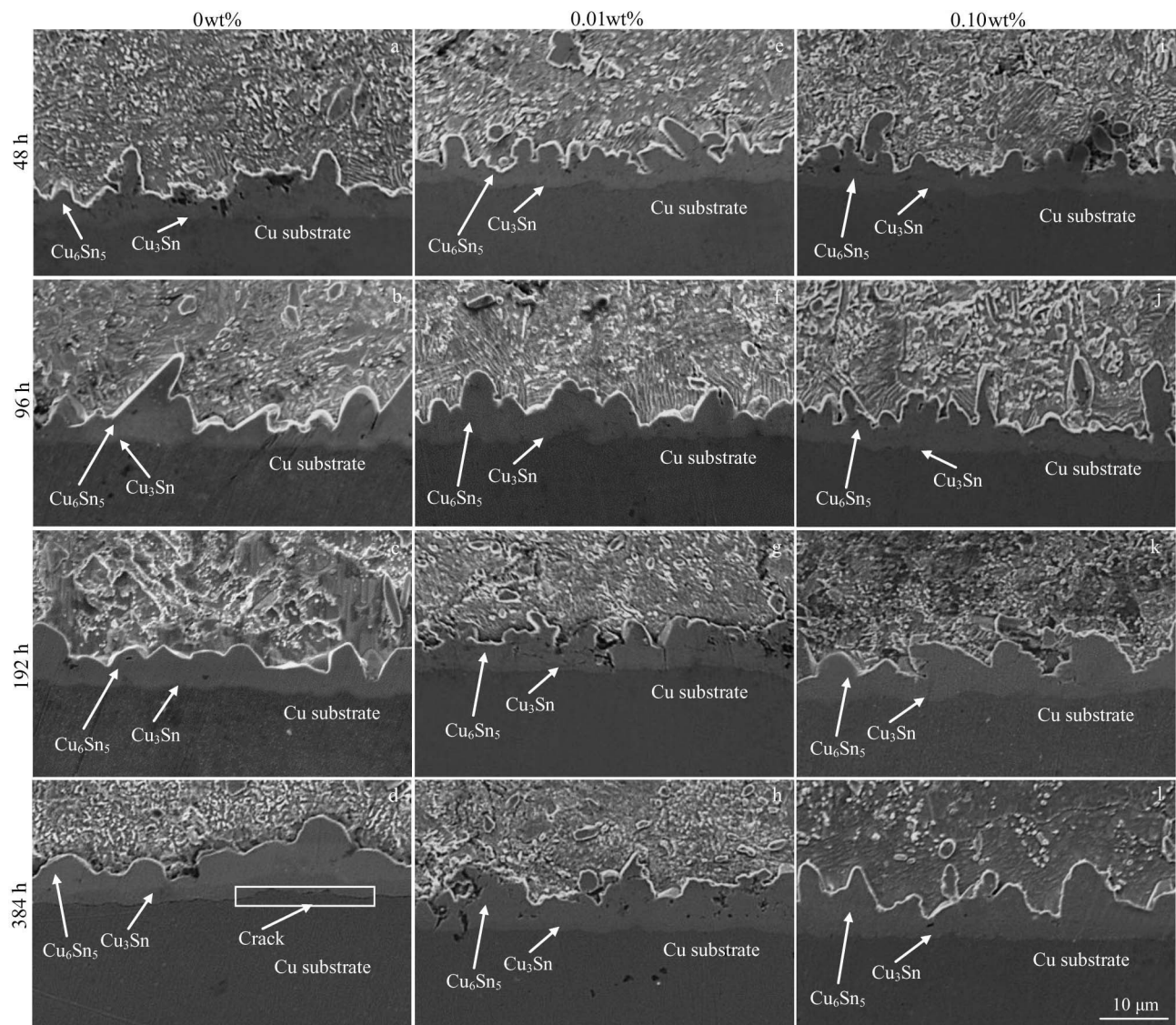


Fig.3 Interface morphologies of Sn2.5Ag0.7Cu0.1RE0.05Ni-xGNSs/Cu soldering joints containing 0wt% GNSs (a–d), 0.01wt% GNSs (e–h), and 0.10wt% GNSs (i–l) after thermal aging for 48 h (a, e, i), 96 h (b, f, j), 192 h (c, g, k), and 384 h (d, h, l)

interface of the soldering joint without GNS addition, whose thickness accounts for about 1/3 of the thickness of IMC layer, as shown in Fig. 3d. Besides, holes and cracks are initiated between the  $\text{Cu}_3\text{Sn}$  layer and the Cu substrate.

Goldmann et al.<sup>[22]</sup> studied the motion law of Cu-Sn diffusion couple by element labeling method. At a relatively low temperature (20–70 °C), Cu in the diffusion couple is the main diffusion element at the interface, and it moves towards Sn side by grain boundary diffusion and gap diffusion. When the aging temperature is higher than 150 °C, Sn will replace Cu as the main diffusion element at the interface and move towards Cu through vacancy diffusion and bulk diffusion. During the thermal aging, the growth of  $\text{Cu}_6\text{Sn}_5$  at the interface mainly depends on the mutual diffusion of Sn atoms in the solder and Cu atoms in the Cu substrate, i.e., the Cu atoms in the substrate pass through IMC layer and react with Sn atoms at the soldering joint/ $\text{Cu}_6\text{Sn}_5$  interface, which thickens the IMC layer. Thus, the Cu atoms reach the

soldering joint, and the interface roughness increases. At the same time, Cu atoms also react with IMC layer to form  $\text{Cu}_3\text{Sn}$  layer during the Cu diffusion to IMC layer. With the thermal aging further proceeding,  $\text{Cu}_3\text{Sn}$  layer begins to grow. Due to the brittleness of  $\text{Cu}_3\text{Sn}$ , its thermal expansion coefficient is quite different from that of Cu. Submicron Kirkendall pores often appear in the  $\text{Cu}_3\text{Sn}$  layer and at the  $\text{Cu}_3\text{Sn}/\text{Cu}$  interface, and even cracks are generated.

When the GNS addition amount is 0.01wt%, the interface morphologies of the soldering joint during the thermal aging are shown in Fig. 3e–3h. Compared with the soldering joint without GNS addition, the thickness of the interface IMC layer decreases, especially that of the  $\text{Cu}_3\text{Sn}$  layer near the Cu substrate. Interface IMC thickness reduction can be attributed to two aspects. Firstly, the reinforcement phase GNS is enriched at the interface during soldering process, which reduces the interdiffusion rate of metal atoms at the interface during thermal aging. At the same time, GNSs have high

surface activity and are easy to be adsorbed on the surface of interface IMC particles, preventing the diffusion of Cu, Sn, and other atoms in the soldering joints. Secondly, the remaining GNSs in the soldering joints near the interface will disturb the concentration gradient of Sn atoms in the composite solder and affect the growth of interface IMC layer. Due to the low GNS addition, the growth of IMC layer at the interface is slightly inhibited, and the thickness of IMC layer is increased greatly with the prolongation in thermal aging time. The interface IMC morphologies of the soldering joint with high GNS content (0.1wt%) are shown in Fig.3i–3l. The thickness of the interface IMC layer is slightly larger than that of the soldering joint without GNS addition, and the surface roughness increases, which can be attributed to the irreversible agglomeration phenomenon under the action of Van der Waals force. This result indicates that the GNS addition is excessive. In the soldering process, GNSs are partially separated from the interface and occupy the Ni sites, causing the composition fluctuation inside the composite

solder, promoting the mutual diffusion between Cu and Sn atoms, and resulting in faster growth of IMC layer.

The interface IMC morphologies of soldering joint with GNS addition of 0.03wt%–0.07wt% are shown in Fig.4. It can be seen that the thickness of IMC layer increases during the thermal aging process. Compared with that in the soldering joint without GNS addition, the growth rate of IMC layer in soldering joint with GNS addition significantly reduces, as well as the growth rate of  $\text{Cu}_3\text{Sn}$  layer. The  $\text{Cu}_3\text{Sn}$  layer cannot be clearly identified after the short-time thermal aging. Wang et al<sup>[23]</sup> reported that the growth of  $\text{Cu}_3\text{Sn}$  layer is mainly controlled by the interface reaction, whereas the growth of  $\text{Cu}_6\text{Sn}_5$  layer is controlled by diffusion. When the thickness of interface IMC layer is small,  $\text{Cu}_6\text{Sn}_5$  phase grows relatively fast, which will inhibit the growth of  $\text{Cu}_3\text{Sn}$  phase, so the interface IMC layer is mainly  $\text{Cu}_6\text{Sn}_5$  phase.

With the thermal aging proceeding, the morphology of interface IMC is transformed from scallop-like and short-rod-like shapes to relatively flat lamellar shape, and some IMC

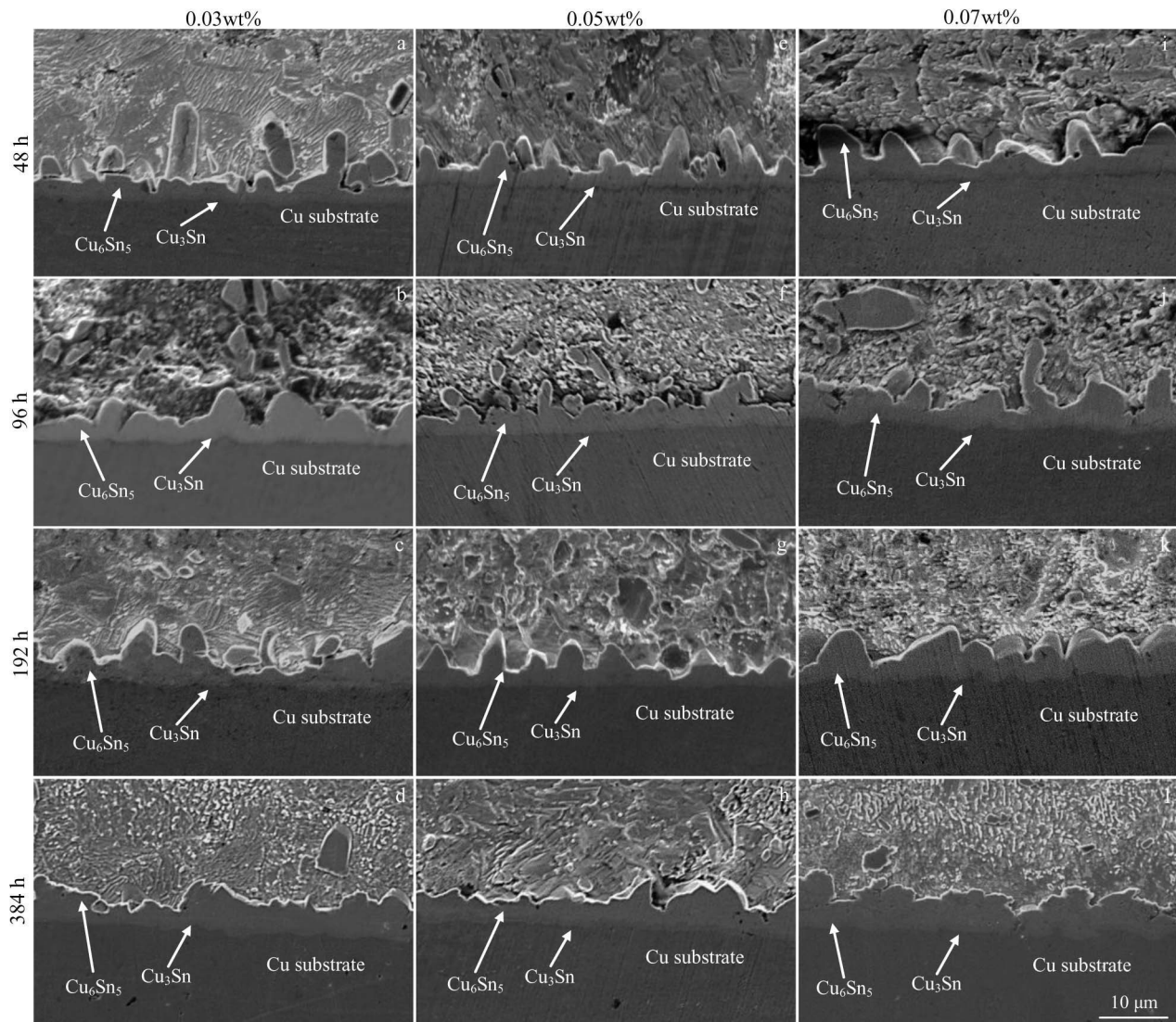


Fig.4 Interface morphologies of Sn<sub>2.5</sub>Ag<sub>0.7</sub>Cu<sub>0.1</sub>RE<sub>0.05</sub>Ni-*x*GNSs/Cu soldering joints containing 0.03wt% GNSs (a–d), 0.05wt% GNSs (e–h), and 0.07wt% GNSs (i–l) after thermal aging for 48 h (a, e, i), 96 h (b, f, j), 192 h (c, g, k), and 384 h (d, h, l)

$\text{Cu}_6\text{Sn}_5$  particles can be observed at the interface between  $\text{Cu}_6\text{Sn}_5$  layer and soldering seam zone at the end of thermal aging, as shown in Fig. 4d and 4l. This is because the Gibbs free energy in the soldering seam zone and interface IMC always decreases during thermal aging process. Scallop-like or rod-like IMCs have large surface area and high surface energy, so the transformation to lamellar-like IMC with low surface energy is necessary for the normal reaction proceeding, which also ensures the stability of the whole system. In addition, when the roughness of interface IMC layer is large, the distance between IMC layer tip and Cu substrate is much greater than the distance between IMC layer groove and Cu substrate. In the thermal aging process, the Cu atoms in the substrate preferentially diffuse to the grooves between IMC particles, promoting the rapid growth of IMC particles and finally flattening the IMC layer. Besides, the grooves between the interface IMCs belong to the near-interface region, where high-density vacancy, dislocation, and other defects are often gathered, and the interface energy is high. Therefore, these regions are used as channels for the quick diffusion of Cu atoms into the solder<sup>[23]</sup>, thus thickening the groove of IMC layer and gradually flattening the interface IMC layer, as shown in Fig. 4d, 4h, and 4l.

Compared with Fig. 3 and Fig. 4, it can be seen that the interface IMC layers with GNS addition of 0.03wt%–0.07wt% are relatively dense with less holes and no cracks. This phenomenon is related to the adsorption of Ni-GNS nanoparticles and other active phases at the interface. According to the surface adsorption theory, the surface energy can be reduced effectively after the surface active materials adsorb on the crystal surface. The Ni-GNS nanoparticles in the composite solder have high surface activity and can be uniformly trapped to the interface during soldering. When the interface spontaneously captures the nano-active phase, the attraction of the atoms inside the solder to the interface metal atoms greatly reduces, which is conducive to the wetting and spreading of the liquid solder on the substrate<sup>[25]</sup>. Additionally, due to the high melting point of Ni-GNSs, Ni-GNSs do not melt in the soldering process, and a frame structure with a certain capillary effect can be formed at the soldering joint, which improves the caulking ability of the liquid solder, avoids the formation of holes to a certain extent, and improves the density of interface IMC layer.

To further study the influence of GNSs on the growth of IMC particles during thermal aging process, the IMC particle size was measured by ImageJ software, as shown in Fig. 5.

With the prolongation of thermal aging time, the particle size of IMC is gradually increased, and the local grain fusion phenomenon appears. According to Oswald grain maturity theory<sup>[26]</sup>, due to different concentrations of Cu atoms in  $\text{Cu}_6\text{Sn}_5$  particles of different sizes which are generated during soldering, a certain concentration gradient is generated among  $\text{Cu}_6\text{Sn}_5$  particles, and Cu atoms will diffuse from small particles with higher concentration to large particles with lower concentration. Eventually, the small  $\text{Cu}_6\text{Sn}_5$  particles contract or even disappear, and only large  $\text{Cu}_6\text{Sn}_5$  particles

exist. Among them, the grain coarsening effect of interface IMC is more obvious without GNS addition. After thermal aging for 96 h, more holes appear in the IMC layer, as shown in Fig. 5b–5d. Tao et al<sup>[27]</sup> studied the effect of alloying elements on the microstructure properties of lead-free soldering joints and found that Ni also has a great influence on the growth of interface IMC. Yoon et al<sup>[28]</sup> found that after the Ni addition, the activation energy of  $(\text{Cu}, \text{Ni})_6\text{Sn}_5$  formation is lower than that of  $\text{Cu}_6\text{Sn}_5$  formation, and the diffusion coefficient of Ni atom in molten Sn is larger than that of Cu atom. As a result, the interdiffusion coefficient of  $(\text{Cu}, \text{Ni})_6\text{Sn}_5$  at the interface increases, and the growth rate of IMC layer is also accelerated during thermal aging.

At the initial stage of thermal aging, the mutual diffusion coefficients of Cu and Sn atoms have a little difference, and no holes are generated at the Cu/Cu<sub>3</sub>Sn interface or IMC layer, as shown in Fig. 5a. This phenomenon indicates that the Cu atoms required for the growth of interface IMC layer at the initial stage of thermal aging mainly come from the supersaturated Cu atoms dissolved in the soldering seam near the interface, and Cu atoms barely diffuse through the Cu substrate. However, the content of Cu atoms in the soldering seam is only 0.7wt%, and Cu atoms are evenly distributed. During soldering, Cu atoms preferentially react with nearby Sn atoms to generate IMC, i. e., Cu atoms are difficult to diffuse to the interface to promote the growth of interface IMC layer. Therefore, before the generation of interface IMC layer, the diffusion process of Sn atoms in the soldering seam zone to the Cu substrate and the dissolution process of Cu atoms in the substrate to the soldering seam occur at the interface, and the Cu atoms near the interface reach the supersaturated state. These supersaturated Cu atoms are gradually precipitated from the soldering seam near the interface and react with Sn atoms to form interface  $\text{Cu}_6\text{Sn}_5$ <sup>[29]</sup>. With the thermal aging proceeding, the oversaturated Cu atoms enriched in the soldering seam near the interface are exhausted. At this time, the growth of interface IMC is mainly caused by the diffusion of Cu atoms in the Cu substrate, and the diffusion rate becomes faster, which promotes the transition from  $\text{Cu}_6\text{Sn}_5$  to  $\text{Cu}_3\text{Sn}$ . At the  $\text{Cu}_3\text{Sn}/\text{Cu}$  interface, vacancy diffusion is dominant, and the diffusion rate of Cu to Sn is much higher than that of Sn to Cu. Therefore, the  $\text{Cu}_3\text{Sn}/\text{Cu}$  interface moves towards the interface of the Cu substrate side and even forms holes (Fig. 5b–5d). These holes remain in the  $\text{Cu}_3\text{Sn}$  layer during interface movement.

Compared with that of interface IMC without GNS addition, the particle size of interface IMC is significantly refined after 0.05wt% GNS addition. In addition to the scalloped IMC particles, a large number of prismatic IMC particles grow towards the soldering seam direction, the holes at the interface decrease, and the interface is rough, as shown in Fig. 5i–5l. This is consistent with the cross-section morphologies of interface IMC in Fig. 4e–4h. Through the investigation on the relationship between joint strength and interface reaction during thermal aging, Kim et al<sup>[30]</sup> found that a flat interface IMC layer can reduce the contact area between

the soldering seam and the interface IMC layer, resulting in the decrease in the bonding strength between the interface IMC and the soldering seam, and ultimately reducing the reliability of joint. Therefore, adding an appropriate amount of GNS can improve the reliability of the joint by changing the shape of interface IMC. During the thermal aging process, the interface IMC gradually flattens, which affects the reliability of the soldering joint.

### 2.3 Interface IMC formation mechanism of composite solder/Cu soldering joint

According to the analysis of interface structure transforma-

tion of soldering joint, the formation of interface IMC includes two stages: reaction and ripening. The first stage is the reaction stage, as shown in Fig.6.

At the initial reaction stage, the solder material is in direct contact with the Cu substrate and generates interface  $Cu_6Sn_5$  IMC, as expressed by Eq.(1):



$Cu_6Sn_5$  grows towards the soldering seam side along the direction perpendicular to the Cu substrate. The growth rate of IMC is determined by the reaction rate. Choi et al<sup>[31]</sup> found that the Jackson factor of  $Cu_6Sn_5$  is less than 2, and the interface is smooth after solidification, i.e., the interface IMC

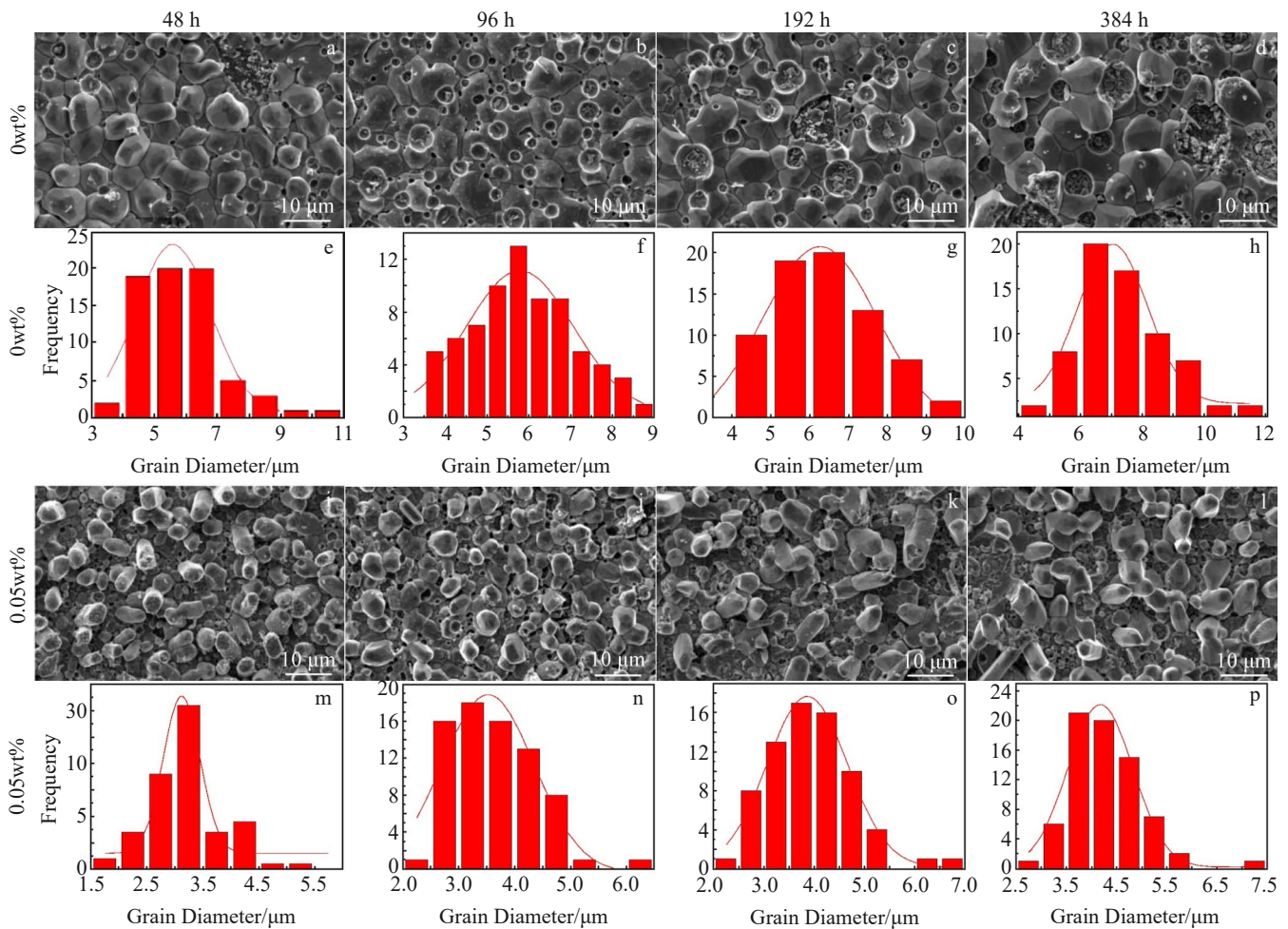


Fig.5 Morphologies (a–d, i–l) and grain diameters (e–h, m–p) of interface IMC grains in Sn2.5Ag0.7Cu0.1RE0.05Ni-xGNSs/Cu soldering joints containing 0wt% GNSs (a–h) and 0.05wt% GNSs (i–p) after thermal aging for 48 h (a, e, i, m), 96 h (b, f, j, n), 192 h (c, g, k, o), and 384 h (d, h, l, p)

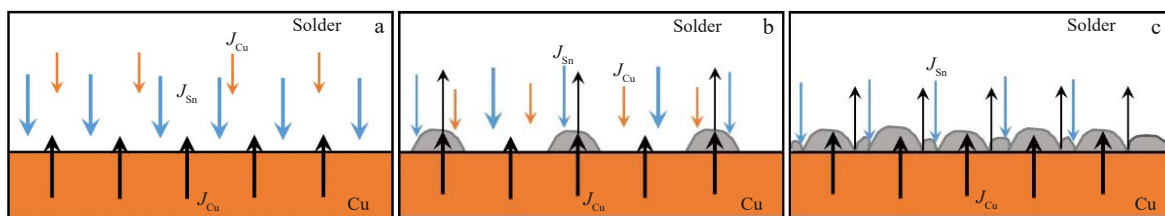


Fig.6 Schematic diagrams of initial (a), middle (b), and end (c) reaction stage

is scalloped.

The growth of IMCs at the interface obstructs the direct contact between Sn and Cu substrate, and Cu atoms need to diffuse through the IMC layer to react with Sn. Therefore, the growth of interface IMC layer is mainly controlled by the diffusion reaction process, and its growth rate depends on the diffusion flux of Cu, as expressed by Eq.(2), as follows:

$$J_{Cu} = D\Delta C/d \quad (2)$$

where  $J_{Cu}$  is the flux diffused from Cu substrate to Sn;  $D$  is the diffusion coefficient of Cu;  $\Delta C$  is the Cu concentration difference between Cu substrate and Cu solder;  $d$  is the thickness of IMC layer.

According to Eq. (2), the diffusion flux of Cu decreases after the formation of IMC. When the interface IMCs are in contact with each other and gradually form a continuous thin layer covering the Cu substrate, diffusion only occurs in the microscopic gaps between the grains, suggesting that the diffusion becomes more and more difficult. With the growth of IMC grains, the atomic diffusion channels between grains are completely blocked.

According to the principle of minimum Gibbs free energy, small grains dissolve and large grains grow. Therefore, IMC enters the second stage, namely the ripening stage, as shown in Fig. 7. Because the saturation solubility of Cu atoms in  $Cu_6Sn_5$  particles of different sizes is different, smaller grains have larger saturation solubility in the parent phase  $\alpha$ . Thus, the Cu atoms diffuse from small particles with radius  $R_2$  to large particles with radius  $R_1$ , and the large particles merge with the small particles and grow up. The driving force of diffusion comes from the concentration difference of parent phase around the small and large particles. As shown in Fig.7a, the free energy of large particles is lower than that of small particles. According to the common tangent rule, the parent phase concentration  $C_{R_1}$  in equilibrium with large particles is lower than that ( $C_{R_2}$ ) in equilibrium with small grains, resulting in the dissolution of small particles and the growth of large particles, as shown in Fig.7b.

#### 2.4 Interface IMC growth kinetics of composite solder/Cu soldering joint

The growth characteristics of interface IMC layer during thermal aging have an important influence on the reliability of

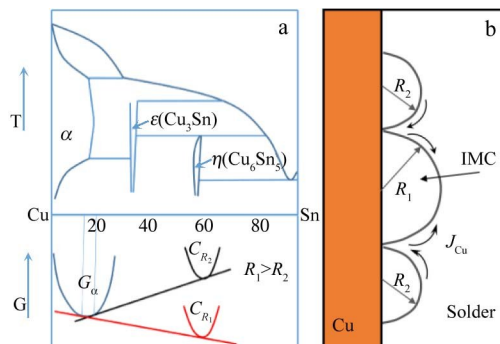


Fig.7 Schematic diagrams of ripening stage: (a) free energy-component relation curves; (b) grain consolidation and growth

soldering joints. Within the thermal aging duration in this research, the growth rate of IMC layer becomes slower due to the GNS addition into the composite solder, and the thickness of  $Cu_3Sn$  layer is smaller than that of the  $Cu_6Sn_5$  IMC layer. Therefore, the growth kinetics of the total interface IMC layer should be further analyzed and discussed. The variation curves of thickness of interface IMC layer with thermal aging time are shown in Fig.8. It can be seen that during the thermal aging process, the thickness of IMC layer increases, basically conforming to the parabolic law. The relationship between the growth change behavior of interface IMC and the thermal aging time can be described by the power-law formula<sup>[32]</sup>, as expressed by Eq.(3), as follows:

$$x(t) = x_0 + (Dt)^n \quad (3)$$

where  $t$  is the thermal aging time;  $x(t)$  is the thickness of interface IMC layer after thermal aging for  $t$  time;  $x_0$  is the thickness of IMC layer before thermal aging;  $D$  is the IMC growth coefficient;  $n$  is the time exponent.

The  $n$  value of interface reaction between solder material and metal substrate is 0.33 – 0.70, and different  $n$  values indicate different growth mechanisms of interface IMC. For example, for parabolic growth with  $n$  value close to 0.5, the growth of interface IMC is mainly controlled by diffusion<sup>[33]</sup>, and the IMC layer grows slowly.

In this research, the growth of interface IMC layer during thermal aging is mainly controlled by volume diffusion, i.e., the growth of interface IMC layer depends on the diffusion of Cu (Ni) and Sn atoms at the interface between solder material and Cu substrate. The growth of IMC layer at the interface obeys the time square root law, i.e., the  $n$  value in Eq.(3) is 0.5. Therefore, the relationship curves between the thickness of IMC layer and the square root of the thermal aging time  $t^{1/2}$  can be obtained, as shown in Fig.8c–8d. In this case, the slope of the growth rate curve of interface IMC is  $D^{1/2}$ . The growth coefficients and linearities of interface IMC layer with different GNS addition amounts obtained from this curve are shown in Table 1.

Based on Table 1, compared with that of interface IMC in soldering joint without GNS addition, the growth coefficient of interface IMC in soldering joint with GNS addition is relatively low. Particularly, when GNS addition amount is 0.03wt%–0.07wt%, the growth coefficient of the interface IMC is about 1/3 of that in soldering joint without GNS addition. These results all suggest that adding an appropriate amount of GNS to the solder can effectively inhibit the growth of interface IMC during thermal aging process, which is also conducive to improve the reliability of soldering joint.

In order to investigate the coarsening mechanism of interface IMC grains during thermal aging, the relationships between particle sizes of interface IMC with thermal aging time are shown in Fig.9.

The power-law formula can also be used to describe the relationship between the coarsening behavior of interface IMC grains and the thermal aging time during the thermal aging process, as shown in Eq.(4):

$$d(t) = d_0 + (Kt)^n \quad (4)$$

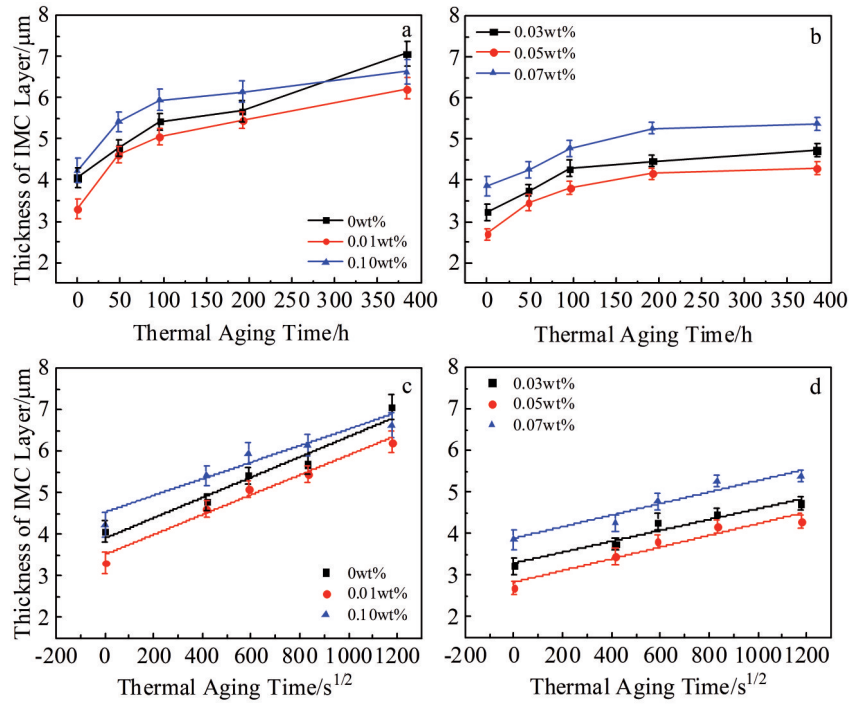


Fig.8 Relationships between thickness of IMC layer in Sn<sub>2.5</sub>Ag<sub>0.7</sub>Cu<sub>0.1</sub>RE<sub>0.05</sub>Ni-*x*GNSs/Cu soldering joints and thermal aging time: (a, c) 0wt% GNSs, 0.01wt% GNSs, and 0.10wt% GNSs; (b, d) 0.03wt% GNSs, 0.05wt% GNSs, and 0.07wt% GNSs

**Table 1 Growth coefficients and linearities of interface IMC in Sn<sub>2.5</sub>Ag<sub>0.7</sub>Cu<sub>0.1</sub>RE<sub>0.05</sub>Ni-*x*GNSs/Cu soldering joints during thermal aging**

Composite solder	Growth coefficient, $D/\times 10^{-14} \text{ cm}^2 \cdot \text{s}^{-1}$	Linearity, $R^2$
Sn <sub>2.5</sub> Ag <sub>0.7</sub> Cu <sub>0.1</sub> RE <sub>0.05</sub> Ni	6.00	0.94
Sn <sub>2.5</sub> Ag <sub>0.7</sub> Cu <sub>0.1</sub> RE <sub>0.05</sub> Ni-0.01GNSs	5.76	0.97
Sn <sub>2.5</sub> Ag <sub>0.7</sub> Cu <sub>0.1</sub> RE <sub>0.05</sub> Ni-0.03GNSs	1.93	0.93
Sn <sub>2.5</sub> Ag <sub>0.7</sub> Cu <sub>0.1</sub> RE <sub>0.05</sub> Ni-0.05GNSs	1.72	0.91
Sn <sub>2.5</sub> Ag <sub>0.7</sub> Cu <sub>0.1</sub> RE <sub>0.05</sub> Ni-0.07GNSs	1.99	0.87
Sn <sub>2.5</sub> Ag <sub>0.7</sub> Cu <sub>0.1</sub> RE <sub>0.05</sub> Ni-0.1GNSs	4.00	0.86

where  $t$  is aging time;  $d(t)$  is the particle size of interface IMC after thermal aging for  $t$  time;  $d_0$  is the particle size of interface IMC before aging;  $K$  is the grain growth coefficient of interface IMC;  $n$  is the time exponent.

According to FDR model<sup>[34]</sup>, the growth of interface Cu<sub>6</sub>Sn<sub>5</sub> grains is determined by the ripening process caused by bulk diffusion in the solder, and there is a linear relationship between the interface Cu<sub>6</sub>Sn<sub>5</sub> particle size and the cube root of the thermal aging time. This means that the relationship between average grain size and the thermal aging time obeys the 1/3 power-law. The relationship between average particle diameter and  $t^{1/3}$  is shown in Fig. 9b, presenting the linear relationship. This result is consistent with the theoretical analysis of the coarsening mechanism of Cu<sub>6</sub>Sn<sub>5</sub> grains in Ref. [24]. The slope of the relationship curve is  $K^{1/3}$ . The growth coefficients and linearities of IMC grains of the

soldering joints obtained from Fig.9 are shown in Table 2.

There is a good linear correlation between IMC particle size and the cubic root of thermal aging time. The growth rate of Cu<sub>6</sub>Sn<sub>5</sub> grains at the interface of composite solder with GNS addition is much slower than that at the interface of solder matrix, indicating that adding appropriate amount of GNS to

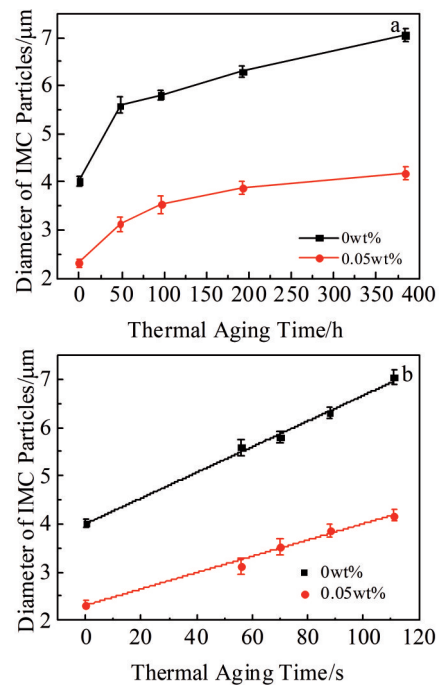


Fig.9 Relationships between particle size of interface IMC in Sn<sub>2.5</sub>Ag<sub>0.7</sub>Cu<sub>0.1</sub>RE<sub>0.05</sub>Ni-*x*GNSs/Cu soldering joints ( $x=0, 0.05$ ) and thermal aging time

**Table 2** Growth coefficients and linearities of IMC particles in Sn2.5Ag0.7Cu0.1RE0.05Ni-xGNSs/Cu soldering joints during thermal aging

Composite solder	Growth coefficient, $K/\times 10^{-17} \text{ cm}^2 \cdot \text{s}^{-1}$	Linearity, $R^2$
Sn2.5Ag0.7Cu0.1RE0.05Ni	1.9	0.996
Sn2.5Ag0.7Cu0.1RE0.05Ni-0.05GNSs	0.48	0.993

the Sn2.5Ag0.7Cu0.1RE0.05Ni solder can effectively inhibit the coarsening of interface IMC grains during the thermal aging process. The GNS addition is beneficial to improve the reliability of soldering joints.

### 2.5 Fracture mechanism of composite solder/Cu soldering joint during thermal aging

The relationships between shear strength of soldering joints and thermal aging time are shown in Fig. 10. It can be seen that adding GNS can improve the shear strength of soldering joints to some extent.

With the prolongation of thermal aging time, the grains of interface IMC are coarsened, presenting a parabolic law. The shear strength of Sn2.5Ag0.7Cu0.1RE0.05Ni-0.05GNSs/Cu soldering joint is 29.53 MPa, which is higher than that of Sn2.5Ag0.7Cu0.1RE0.05Ni/Cu soldering joint by 23.5%. The main reason is that the uniform distribution of reinforcement phase particles inhibits the growth of IMC grains in the soldering seam and the solder. The fine IMC grains hinder the dislocation slip along the shear direction through the pinning effect. In addition, the thermal mismatch between reinforcement phase and solder matrix and the load transfer of reinforcement phase involved in Ref. [8] can also be used to explain the increase in shear strength of the soldering joints. However, with the further increase in GNS addition amount, the shear strength of the soldering joint is decreased to some extent. This phenomenon is related to the stress concentration in the soldering joint caused by agglomerated GNSs in the composite solder.

According to Fig. 10, the shear strength of soldering joints is decreased with the prolongation of aging time. It can be seen that the shear strength of Sn2.5Ag0.7Cu0.1RE0.05Ni/Cu

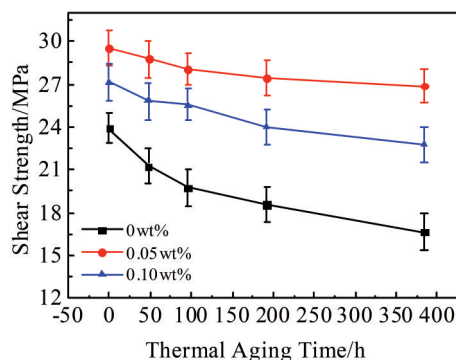


Fig.10 Relationship between shear strength and thermal aging time of Sn2.5Ag0.7Cu0.1RE0.05Ni-xGNSs/Cu soldering joints

soldering joint decreases greatly from 23.92 MPa (before thermal aging) to 16.63 MPa (after thermal aging), which decreases by 30.5%. This degradation is related to the Coriolis effect and micro-cracks caused by stress concentration during thermal aging<sup>[35]</sup>. As shown in Fig. 3d, the micro-cracks can be observed at the Cu<sub>3</sub>Sn/Cu interface after thermal aging for 384 h, resulting in a significant reduction in shear strength. After adding GNSs, the shear strength decrement of composite soldering joints is less. Particularly, when GNS addition is 0.05wt%, the shear strength only decreases by 8.9%. After thermal aging for 96 h, the shear strength tends to be stable. After thermal aging for 384 h, the shear strength is still higher than that of the Sn2.5Ag0.7Cu0.1RE0.05Ni/Cu soldering joint before aging. These results indicate that the addition of GNSs cannot only greatly improve the shear strength of soldering joints, but also effectively inhibit the decrease in shear strength during the thermal aging process, which is conducive to the improvement in reliability of soldering joints.

In order to further analyze the effect of GNS addition on the shear strength of soldering joints during the thermal aging process, the shear fracture morphologies of the soldering joint are shown in Fig. 11. It can be seen from Fig. 11 that before thermal aging, the fracture of Sn2.5Ag0.7Cu0.1RE0.05Ni/Cu and Sn2.5Ag0.7Cu0.1RE0.05Ni-0.05GNSs/Cu soldering joints both occurs in the soldering seam zone. The shear fracture of the Sn2.5Ag0.7Cu0.1RE0.05Ni/Cu soldering joint is composed of parabolic dimples and cleavage steps (Fig. 11a), and a small number of IMC particles can also be observed, which belongs to the tough-brittle mixed fracture.

The shear fracture of the Sn2.5Ag0.7Cu0.1RE0.05Ni-0.05GNSs/Cu soldering joint presents the typical parabolic dimples (Fig. 11b), and the dimple size is large, which belongs to the ductile fracture. As shown in the inset of Fig. 11b, in the dimple root, a translucent crumpled material with a slice diameter of 10–20  $\mu\text{m}$  appears, which is a typical feature of GNSs. It can be inferred that GNSs are distributed in the soldering seam zone or at the interface between soldering seam and interface IMC layer, which can inhibit the growth of IMC particles and the thickening of the interface IMC layer. These results are beneficial to increase the shear strength of composite soldering joints. After thermal aging for 192 h, the shear fracture morphology of Sn2.5Ag0.7Cu0.1RE0.05Ni/Cu soldering joint shows the parabolic dimples and cleavage plane, and there are large pebble-like pits at the dimple root, which are traces left after the interface IMC grains are pulled out during the shear process. Therefore, the fracture location moves from the soldering seam zone to the soldering seam/IMC layer, which is accompanied by the breakage and fracture of some IMC grains, indicating the brittle fracture. Consequently, the shear strength is greatly reduced.

The shear fracture of the composite soldering joint with 0.05wt% GNS addition after thermal aging for 192 h is composed of parabolic dimples and cleavage planes, as shown in Fig. 11d. Compared with the fracture morphology of the soldering joint before thermal aging, the dimple size is reduced, the fracture fluctuation is larger, and no interface

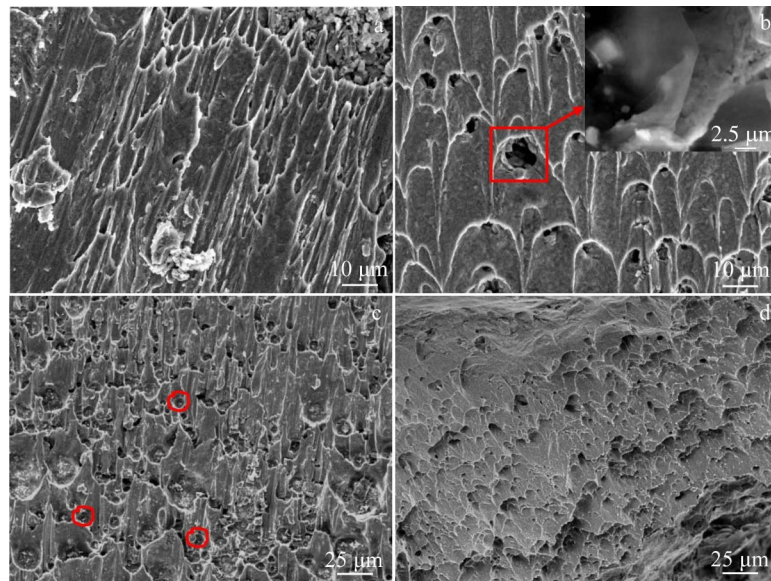


Fig.11 Shear fracture morphologies of Sn2.5Ag0.7Cu0.1RE0.05Ni/Cu (a, c) and Sn2.5Ag0.7Cu0.1RE0.05Ni-0.05GNSs/Cu (b, d) soldering joints after thermal aging for 0 h (a–b) and 192 h (c–d)

IMC particles can be found. The fracture location is still in the soldering seam zone, and the shear strength is relatively high. This is because the interface IMC layer with 0.05wt% GNS addition only accounts for a small part in the soldering joint, the fracture behavior is controlled by the solder, and the ductile fracture is dominant. However, Sn2.5Ag0.7Cu0.1RE-0.05Ni/Cu soldering joint contains more interface IMCs, the fracture behavior is controlled by IMC, and the brittle fracture mode is dominant<sup>[36]</sup>.

In conclusion, during the thermal aging process, the fracture position of Sn2.5Ag0.7Cu0.1RE0.05Ni/Cu soldering joint shifts from the soldering seam zone to the soldering seam/IMC layer, and the shear strength of the soldering joint decreases greatly. The fracture locations of the soldering joint with 0.05wt% GNS addition are all in the soldering seam zone. Ni in the composite solder can hardly be ionized due to strong chemisorption with GNSs, and the surface active GNSs tend to be adsorbed by IMC particles, which inhibits the growth of IMC particles and thus inhibits the significant reduction in shear strength of the soldering joints during thermal aging.

### 3 Conclusions

1) SnAgCuRE system composite solder reinforced by Ni-GNSs is mainly composed of  $\beta$ -Sn, Ag<sub>3</sub>Sn, and a small amount of Cu<sub>6</sub>Sn<sub>5</sub>. The addition of Ni-GNSs inhibits the linear expansion of the composite solder, resulting in lattice distortion and dislocation. IMC particles near the dislocation line interact with the dislocation and hinder the dislocation movement, therefore strengthening the composite solder. Then, the composite soldering joint is also strengthened. The interface IMC of the composite soldering joint is pebble-like and rod-like. When GNS addition amount is 0.03wt%–0.07wt%, the thickness of the interface IMC layer is small, and the IMC grains and soldering seam microstructure are refined.

2) The thickness of IMC layer increases during the thermal aging, and Sn2.5Ag0.7Cu0.1RE0.05Ni/Cu soldering joint has the largest thickness increment. The Cu<sub>3</sub>Sn IMC layer is obvious, and there are Kirkendall holes and micro-cracks at the IMC layer/Cu interface. The growth coefficients of IMC layer and IMC particles of composite soldering joints decrease significantly when GNS addition amount is 0.03wt%–0.07wt%, indicating that the growth of interface IMC is effectively inhibited by adding appropriate GNSs.

3) Adding an appropriate amount of GNS can effectively alleviate the decrease in mechanical properties of composite soldering joints during the thermal aging. The shear strength reduction of composite soldering joint with 0.05wt% GNS addition is the minimum of 8.9%. After thermal aging for 384 h, its shear strength is still higher than that of the Sn2.5Ag-0.7Cu0.1RE0.05Ni/Cu soldering joint before thermal aging. The fracture position of Sn2.5Ag0.7Cu0.1RE0.05Ni/Cu soldering joint shifts from the soldering seam zone to the soldering seam/IMC layer, whereas the fracture locations of the soldering joint with 0.05wt% GNS addition are all in the soldering seam zone, which suggests higher shear strength.

### References

- 1 Kim K S, Huh S H, Suganuma K. *Microelectron Reliability*[J], 2003, 43(2): 259
- 2 Zhong Y, Liu W, Wang C Q et al. *Materials Science and Engineering A*[J], 2016, 652: 264
- 3 Kumar K M, Kripesh V, Tay A A O. *Journal of Alloys and Compounds*[J], 2008, 450: 229
- 4 Xin M L, Wang X Q, Sun F L. *Journal of Materials Science: Materials in Electronics*[J], 2022, 33: 25025
- 5 Yang L M, Lu X L, Mu G W. *Materials Today Communications*[J], 2022, 32: 104025

- 6 Yang W R, Ding Y, Liao M Q et al. *Journal of Materials Science: Materials in Electronics*[J], 2022, 33: 17137
- 7 Wang B Y, Wu Y J, Wu W et al. *Journal of Materials Science*[J], 2022, 57: 17491
- 8 Wang H G, Zhang K K, Wu Y J et al. *Journal of Materials Science: Materials in Electronics*[J], 2021, 32: 28695
- 9 Jiang N, Zhang L, Xu K K et al. *Rare Metal Materials and Engineering*[J], 2021, 50(7): 2293
- 10 Han Y D, Jing H Y, Wang L X et al. *Journal of Alloys and Compounds*[J], 2015, 650: 475
- 11 Jing H Y, Guo H J, Wang L X et al. *Journal of Alloys and Compounds*[J], 2017, 702: 669
- 12 Park B G, Myung W R, Lee C J et al. *Composites Part B*[J], 2020, 182: 107617
- 13 Aamir M, Muhammad R, Ahmed N et al. *Microelectron Reliability*[J], 2017, 78: 311
- 14 Hu X W, Xu T, Jiang X X et al. *Applied Physics A*[J], 2016, 122: 278
- 15 Xu T, Hu X W, Li J Y et al. *Journal of Materials Science: Materials in Electronics*[J], 2020, 31: 3876
- 16 Liang S B, Ke C B, Huang J Q et al. *Microelectron Reliability*[J], 2019, 92: 1
- 17 Wan Y Q, Hu X W, Xu T et al. *Microelectron Engineering*[J], 2018, 199: 69
- 18 Suganuma K. *Current Opinion in Solid State and Materials Science*[J], 2001, 5(1): 55
- 19 Yoon D, Son Y W, Cheong H. *Nanoscience and Nanotechnology Letters*[J], 2011, 11: 3227
- 20 Liu X D, Han Y D, Jing H Y et al. *Materials Science and Engineering A*[J], 2013, 562: 25
- 21 Pu C J, Li C J, Peng J B et al. *Rare Metal Materials and Engineering*[J], 2023, 52(9): 3302
- 22 Goldmann L S. *ASME International Mechanical Engineering Congress and Exposition*[J], 1996, 15397: 169
- 23 Wang Man, Yu Zhishui, Zhang Peilei et al. *Materials Reports*[J], 2015, 29(23): 148 (in Chinese)
- 24 Kim H K, Tu K N. *Physical Review B*[J], 1996, 53(23): 16027
- 25 Wang H G, Zhang K K, Wu Y J et al. *Materials & Design*[J], 2021, 212: 110222
- 26 Gusak A M, Chen C, Tu K N. *Philosophical Magazine*[J], 2016, 96(13): 1318
- 27 Tao Q B, Benabou L, Vivet L et al. *Materials Science and Engineering A*[J], 2016, 669: 403
- 28 Yoon J W, Lee C B, Kim D U et al. *Metals and Materials International*[J], 2003, 9: 193
- 29 Li H L, An R, Wang C Q et al. *Journal of Alloys and Compounds*[J], 2015, 634: 94
- 30 Kim D G, Jang H S, Kim J W et al. *Journal of Materials Science: Materials in Electronics*[J], 2005, 16: 603
- 31 Choi S, Bieler T R, Lucas J P et al. *Journal of Electronic Materials*[J], 1999, 28: 1209
- 32 Shen J, Zhao M L, He P P et al. *Journal of Alloys and Compounds*[J], 2013, 574: 451
- 33 Zhou Minbo, Ma Xiao, Zhang Xinping. *Acta Metallurgica Sinica*[J], 2013, 49(3): 341 (in Chinese)
- 34 Gusak A M, Tu K N. *Physical Review B*[J], 2002, 66: 115403
- 35 Wu C D, Liu K W, Cheng P C. *Applied Physics A*[J], 2023, 129: 255
- 36 Hu X W, Chen W J, Yu X et al. *Journal of Alloys and Compounds*[J], 2014, 600: 13

## Ni改性GNSs对SnAgCuRE/Cu钎焊接头热老化特性的影响

王悔改<sup>1,2</sup>, 张柯柯<sup>1,2</sup>, 王冰莹<sup>1</sup>, 王要利<sup>1,2</sup>

(1. 河南科技大学 材料科学与工程学院, 河南 洛阳 471023)

(2. 有色金属新材料与先进加工技术省部共建协同创新中心 有色金属共性技术河南省协同创新中心, 河南 洛阳 471023)

**摘要:** 以Sn<sub>2.5</sub>Ag<sub>0.7</sub>Cu<sub>0.1</sub>RE<sub>0.05</sub>Ni无铅钎料合金为研究对象, 基于石墨烯纳米片(GNS)独特的结构、优异的物理性能和力学性能, 以其为复合钎料的增强相, 开展基于Ni改性GNSs(Ni-GNSs)增强SnAgCuRE系复合钎料/Cu的钎焊和钎焊接头热老化试验, 探讨Ni-GNSs对复合钎料组织及钎焊接头热老化失效断裂机制的影响。结果表明: Ni-GNSs的加入, 抑制了复合钎料的线膨胀, 产生晶格畸变, 导致位错产生, 金属间化合物(IMC)颗粒分布在位错线附近, 与位错发生交互作用, 阻碍位错运动, 强化复合钎料, 进而强化复合钎料接头。随着热老化时间延长, 钎焊接头界面IMC层厚度增加, 剪切强度降低; 其中, 添加0.05%(质量分数)GNSs的复合钎料接头剪切强度降幅最小, 为8.9%, 且热老化384 h后, 其剪切强度仍高于Sn<sub>2.5</sub>Ag<sub>0.7</sub>Cu<sub>0.1</sub>RE<sub>0.05</sub>Ni/Cu合金接头热老化前的剪切强度。Ni-GNSs的加入, 使复合钎料钎焊接头界面IMC的生长系数明显降低, 有效缓解了复合钎料/Cu钎焊接头热老化过程中力学性能的降低, 进而改变复合钎料/Cu钎焊接头的热老化失效断裂机制, 最终影响接头的可靠性。Sn<sub>2.5</sub>Ag<sub>0.7</sub>Cu<sub>0.1</sub>RE<sub>0.05</sub>Ni/Cu钎焊接头的断裂位置由热老化前的钎缝区向钎缝/界面IMC移动, 变为韧脆混合断裂; 而添加0.05%(质量分数)GNSs复合钎料接头的断裂位置均在钎缝区, 为韧性断裂, 钎焊接头可靠性较高。

**关键词:** Ni-GNSs/SnAgCuRE系复合钎料; 界面IMC; 钎焊接头; 热老化; 组织与性能

作者简介: 王悔改, 女, 1980年生, 博士, 副教授, 河南科技大学材料科学与工程学院, 河南 洛阳 471023, 电话: 0379-64231269, E-mail: 9902783@haust.edu.cn